Joint optimization of learning-based image reconstruction and k-space trajectories for MRI

Jeffrey A. Fessler

EECS Department, BME Department, Dept. of Radiology
University of Michigan

`http://web.eecs.umich.edu/~fessler`

Duke University Center for Virtual Imaging Trials
2022-10-21

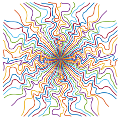

Brain

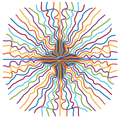

Knee

Acknowledgments:
Guanhua Wang, Tianrui Luo, Jon Nielsen, Doug Noll

Outline

Outline

Medical imaging overview

Design Scan $\rightarrow$ Acquire Data $\xrightarrow{\boldsymbol{y}}$ Reconstruct Images $\xrightarrow{\hat{\boldsymbol{x}}}$ Process Images $\rightarrow$ Diagnose Interpret

raw data ($\boldsymbol{y}$) — images ($\hat{\boldsymbol{x}}$)

Medical imaging overview

raw data $\qquad\qquad$ images

Design Scan $\rightarrow$ Acquire Data $\xrightarrow{\boldsymbol{y}}$ Reconstruct Images $\xrightarrow{\hat{\boldsymbol{x}}}$ **Process Images** $\rightarrow$ Diagnose Interpret

Most obvious place for machine learning is in post-processing (image analysis).
Numerous special issues and surveys in medical imaging journals, *e.g.*, [1–9].

Medical imaging overview

raw data $\qquad\qquad$ images

Design Scan $\rightarrow$ Acquire Data $\xrightarrow{\boldsymbol{y}}$ Reconstruct Images $\xrightarrow{\hat{\boldsymbol{x}}}$ Process Images $\rightarrow$ Diagnose Interpret

Machine learning for scan design (k-space sampling):

- Choose best k-space phase encoding locations (usually Cartesian sampling)
- Uses "ground truth" (fully sampled) training images
- Hot topic in MRI research recently, *e.g.*, [10–15]
- Precursor by Yue Cao and David Levin, MRM Sep. 1993 [16–18]

Medical imaging overview

$$\boxed{\text{Design Scan}} \rightarrow \boxed{\text{Acquire Data}} \xrightarrow[\text{}]{\overset{\text{raw data}}{\boldsymbol{y}}} \boxed{\text{Reconstruct Images}} \xrightarrow{\overset{\text{images}}{\hat{\boldsymbol{x}}}} \boxed{\text{Process Images}} \rightarrow \boxed{\text{Diagnose Interpret}}$$

Machine learning in medical image reconstruction:

- June 2018 special issue of IEEE Trans. on Medical Imaging [19].
- Surveys: [20–27]
- Possibly easier than diagnosis due to lower bar:
  - current reconstruction methods based on simplistic image models;
  - human eyes are better at detection than at solving inverse problems.

Medical imaging overview

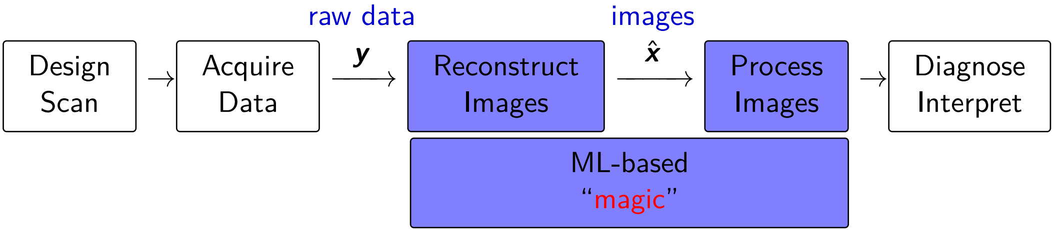

A holy grail for machine learning in medical imaging?

- CT sinogram to vessel diameter [28, 29]
- k-space to ???

Joint optimization of sampling and reconstruction

Design Scan → **Acquire Data** $\xrightarrow[\text{raw data}]{\boldsymbol{y}}$ **Reconstruct Images** $\xrightarrow[\text{images}]{\hat{\boldsymbol{x}}}$ **Process Images** → **Diagnose Interpret**

"B-spline parameterized joint optimization of reconstruction and k-space trajectories (BJORK) for accelerated 2D MRI," arXiv 2101.11369 [30] IEEE T-MI 2022 [31]
Guanhua Wang, T. Luo, J.-F. Nielsen, D. Noll, J. Fessler

Preview:

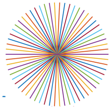

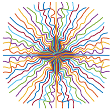

Knee

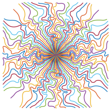

Brain

Related work: "PILOT" by Weiss et al. [32]; J-MoDL work of Aggarwal et al. [14].

MR sampling and under-sampling

All clinical MRI scans currently use "hand-crafted" sampling patterns:

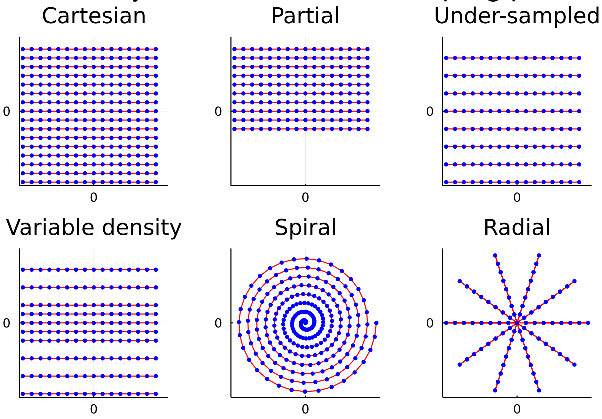

- Reducing k-space sampling $\implies$ reduced scan time / improved temporal resolution
- Under-sampled data benefits from advanced reconstruction methods

Outline

Overview:

- image-domain learning [33–35]...
- k-space or data-domain learning
  e.g., [36], [37], [38]
- transform learning (direct from k-space to image)
  e.g., AUTOMAP [39], [40–42]
- hybrid-domain learning (unrolled loop, *e.g.*, variational network)
  alternate between denoising/dealiasing and reconstruction from k-space
  e.g., [37, 43–47] ...

DL for IR: image-domain learning

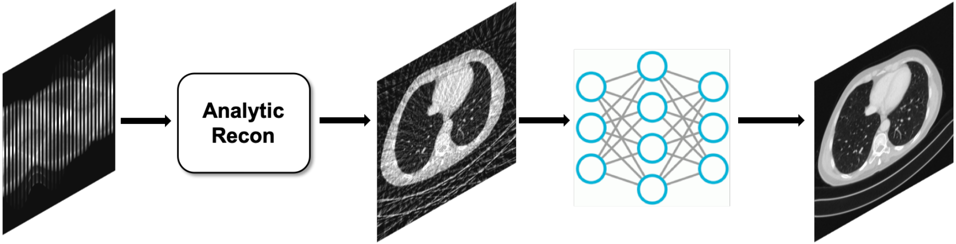

Figure courtesy of Jong Chul Ye, KAIST University.

+ simple and fast
− aliasing is spatially widespread, requires deep network

Investigating Robustness to Unseen Pathologies in Model-Free Deep Multicoil Reconstruction

Gopal Nataraj[1] and Ricardo Otazo[1,2]
[1]Dept. of Medical Physics, Memorial Sloan Kettering Cancer Center
[2]Dept. of Radiology, Memorial Sloan Kettering Cancer Center

Introduction
Speed is often claimed as a key advantage of deep learning (DL) for undersampled parallel MRI reconstruction [1]. However, the only DL approach that to our knowledge has studied generalizability to pathologies unseen in training [2] requires repeated application of the MR acquisition model and its adjoint, just as in iterative methods. In contrast, model-free DL reconstruction has the potential to be much faster. Prior model-free DL work [3] proposes to learn a mapping directly from k-space, but with

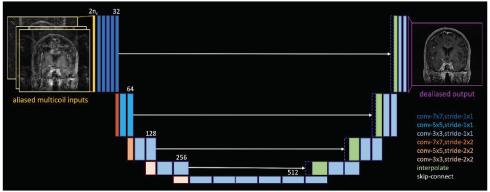

[48] ISMRM 2020 Workshop on Data Sampling & Image Reconstruction

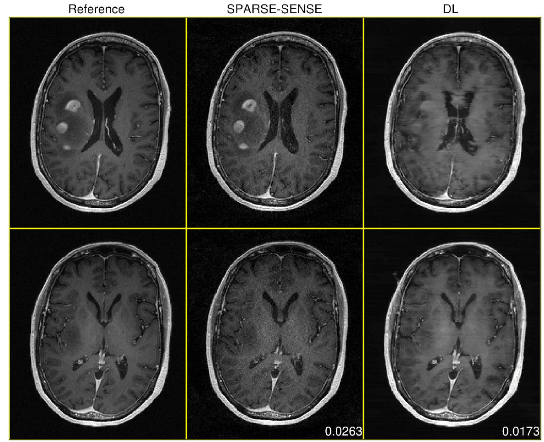

Figure 3: Reconstructions in a case of anaplastic astrocytoma, a rare malignant brain tumor. SPARSE-SENSE and DL reconstructions are from the same 4x-accelerated retrospectively undersampled acquisition. DL achieves lower whole-volume MAE than SPARSE-SENSE, but fails to properly reconstruct regions near the tumor.

- Use NN output as a “prior” for iterative reconstruction [33, 49]:

$$\hat{\boldsymbol{x}}_\beta = \arg\min_{\boldsymbol{x}} \|\boldsymbol{A}\boldsymbol{x} - \boldsymbol{y}\|_2^2 + \beta \, \|\boldsymbol{x} - \boldsymbol{x}_{\mathrm{NN}}\|_2^2 = (\boldsymbol{A}'\boldsymbol{A} + \beta \boldsymbol{I})^{-1}(\boldsymbol{A}'\boldsymbol{y} + \beta \boldsymbol{x}_{\mathrm{NN}})$$

  - For single-coil Cartesian case:
    - no iterations are needed (solve with FFTs)
    - $\lim_{\beta\to 0} \hat{\boldsymbol{x}}_\beta$ replaces missing k-space data with FFT of $\boldsymbol{x}_{\mathrm{NN}}$
  - Iterations needed for parallel MRI and/or non-Cartesian sampling (PCG)

- Learn residual (aliasing artifacts), then subtract [50, 51]

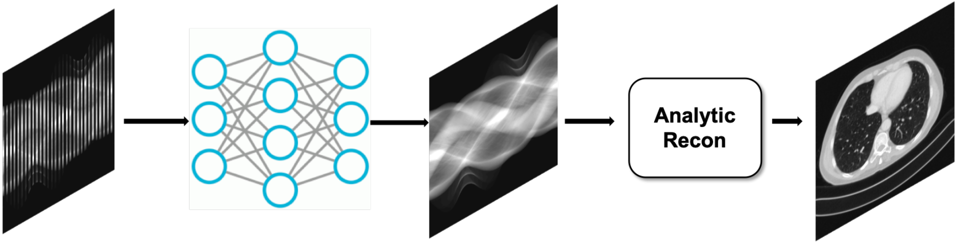

Figure courtesy of Jong Chul Ye, KAIST University.

+ simple and fast ("nonlinear GRAPPA")
+ "database-free" : learn from auto-calibration data [36], [37], [38]
− perhaps harder to represent local image features?

DL for IR: transform learning

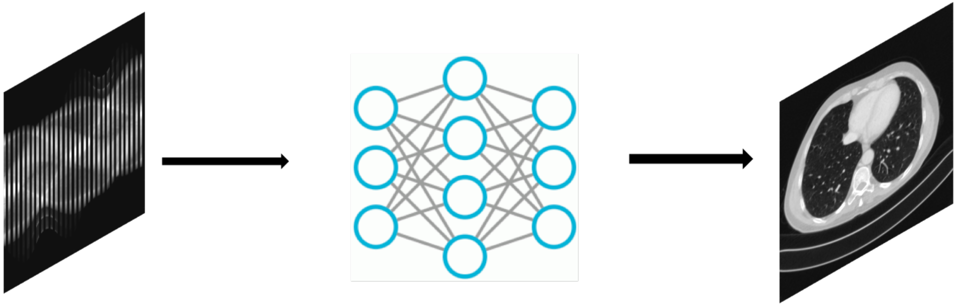

Figure courtesy of Jong Chul Ye, KAIST University.

+ in principle, purely data driven; potential to avoid model mismatch
− high memory requirement for fully connected layers [39]

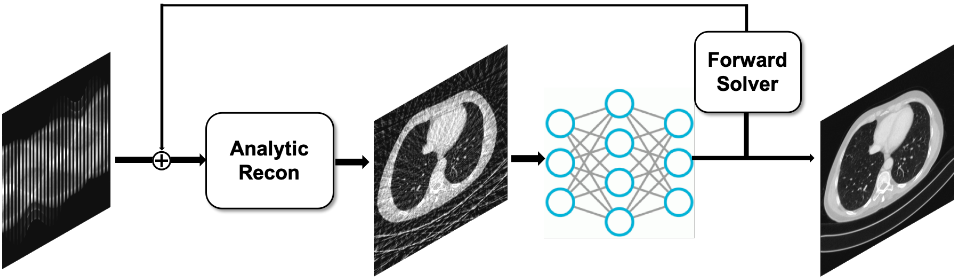

Figure courtesy of Jong Chul Ye, KAIST University.

+ physics-based use of k-space data & image-domain priors, *e.g.*, [37, 43–47, 52, 53] ...
+ interpretable connections to optimization approaches
+ best results in MRI recon challenges [54–56]
− more computation to due to "iterations" (hyper-layers) and repeated $\boldsymbol{A}\boldsymbol{x}$, $\boldsymbol{A}'\boldsymbol{r}$

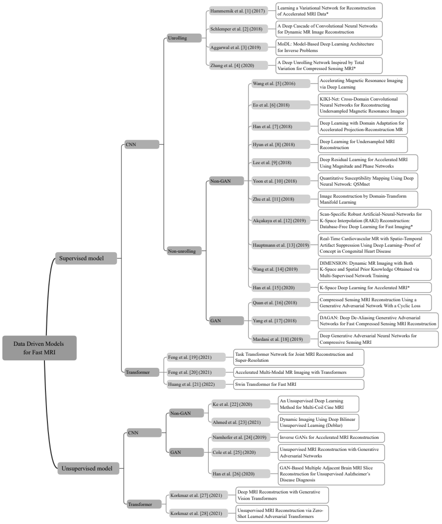

Huang et al.., arXiv 2204.01706, Apr. 2022 [57]

Outline

Learning MRI sampling patterns I

Pre-specified image reconstruction methods

Cartesian sampling pattern optimization

- Yue Cao & David Levin, MRM Sep. 1993 [16–18]
  Feature recognizing MRI
- Seeger et al., MRM 2010 [58]
  Single coil, 1D Cartesian, 2D spiral angles, CS-type recon, Bayesian information gain
- Ravishankar & Bresler, EMBS 2011 [10]
  Single coil, 1D & 2D sampling, DLMRI recon (DL = dictionary learning), weighted k-space loss
- Baldassarre . . . Cevher, IEEE J-STSP 2016 [11]
  Single coil, 2D sampling, energy preserving criterion

Joint learning of sampling and reconstruction

- Gözcü ... Cevher, IEEE T-MI 2018 [12]
  Single coil, 1D sampling, several fixed recon methods (TV, BP, BM3D, image-domain NN), image-domain training loss
- Aggarwal & Jacob IEEE J-STSP 2020 [14] (J-MoDL)
  Multi-coil, 1D (horizontal and vertical) sampling, MoDL recon
- Bahadir ... Sabuncu, IEEE T-CI 2020 [15] (LOUPE)
  Single coil, 1D & 2D sampling, IFFT/U-Net recon
- Weiss et al., arXiv 1909.05773 (2019, 2020, 2021) (PILOT) [32]
  Single coil, Non-Cartesian sampling, IFFT/U-Net recon
- Wang ... Fessler, ISMRM 2021, arXiv 2021 (BJORK) [30, 59]
  Multi-coil, Non-Cartesian sampling, MoDL-type recon
  Fast and efficient DFT Jacobian approximations [60, 61]

Adaptive phase-encode selection

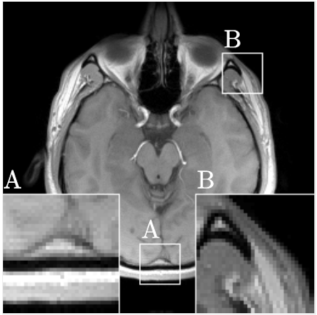

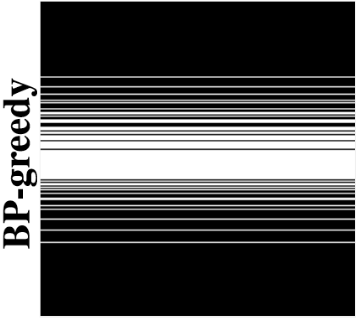

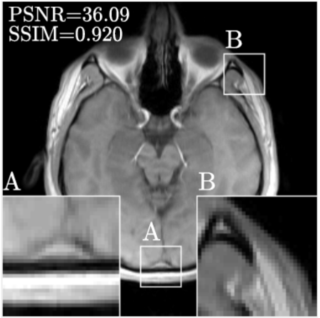

- Sampling designed to optimize PSNR for basis pursuit (BP) reconstruction using shearlet transform, at 25% sampling rate.
- Sampling design considers both the training data and the reconstruction method.
- No high spatial frequencies!?

(Images from Gözcü et al. [12].)

Outline

- MRI measurement model:

$$\boldsymbol{y} = \boldsymbol{A}(\boldsymbol{\omega})\boldsymbol{x} + \boldsymbol{\varepsilon}$$

  - $\boldsymbol{y} \in \mathbb{C}^M$: k-space data; $M \sim 10 - 30\text{K}$
  - $\boldsymbol{\omega} \in \mathbb{R}^{M \times 2}$: k-space sampling pattern ("trajectory"): 2D in this work
  - $\boldsymbol{x} \in \mathbb{C}^N$: unknown true image, $N \sim 100\text{K}$
  - $\boldsymbol{A}(\boldsymbol{\omega}) \in \mathbb{C}^{M \times N}$: encoding matrix (coil sensitivity, etc.)
  - $\boldsymbol{\varepsilon} \in \mathbb{C}^M$: measurement noise
- Reconstruction method:

$$\hat{\boldsymbol{x}} = f(\boldsymbol{y}; \boldsymbol{\omega}, \boldsymbol{\theta})$$

  - $\boldsymbol{\theta}$: model parameters of reconstruction method (e.g., CNN weights)
  - Deep iterative down-up CNN (DIDN) has $\sim$ 165M learned parameters [62]
- Image quality goal:

$$\hat{\boldsymbol{x}} = f(\boldsymbol{y}; \boldsymbol{\omega}, \boldsymbol{\theta}) = f(\boldsymbol{A}(\boldsymbol{\omega})\boldsymbol{x} + \boldsymbol{\varepsilon}; \boldsymbol{\omega}, \boldsymbol{\theta}) \approx \boldsymbol{x}$$

Supervised approach

- Define training loss function such as $\ell(\hat{\boldsymbol{x}}, \boldsymbol{x}) = \|\hat{\boldsymbol{x}} - \boldsymbol{x}\|_1 + \alpha \|\hat{\boldsymbol{x}} - \hat{\boldsymbol{x}}\|_2$
- Select N_{train} fully sampled training images $\boldsymbol{x}_1, \boldsymbol{x}_2, \ldots$
- Jointly optimize k-space trajectory $\boldsymbol{\omega}$ and image reconstruction method $\boldsymbol{\theta}$

$$(\hat{\boldsymbol{\omega}}, \hat{\boldsymbol{\theta}}) = \underset{\boldsymbol{\omega}, \boldsymbol{\theta}}{\arg\min} \frac{1}{N_{\text{train}}} \sum_{n=1}^{N_{\text{train}}} \ell(f(\boldsymbol{A}(\boldsymbol{\omega})\boldsymbol{x}_n + \boldsymbol{\varepsilon}_n; \boldsymbol{\omega}, \boldsymbol{\theta}), \boldsymbol{x}_n)$$

- Details:
  - Reconstruction using MoDL method [52]
  - Can use multiple noise realizations $\boldsymbol{\varepsilon}$ per training image
  - Enforce gradient amplitude and slew-rate limits for $\boldsymbol{\omega}$
  - Use B-spline parameterization of k-space trajectory
  - Coarse-to-fine search of trajectory to avoid poor local minimizers
  - Eddy current correction
  - Fast NUFFT Jacobian approximation [60, 61, 63]

BJORK Diagram

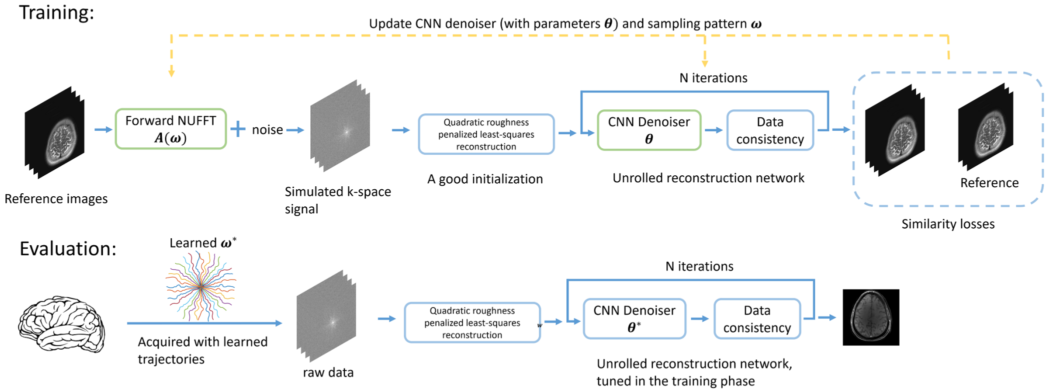

Data

- NYU/FAIR fastMRI brain and knee data
- 16/24/32 radial spokes of 1280 points for trajectory initialization ($\approx$ 10-20 $\times$ acceleration for 320 $\times$ 320 image)
- 22cm FOV, Gmax $=$ 5 Gauss/cm, slew rate $\leq$ 15 Gauss/cm/ms
- 5ms readout duration radial, 16ms spiral
- Comparison with SPARKLING approach of [64] using its default density

Trajectory is tailored to anatomy

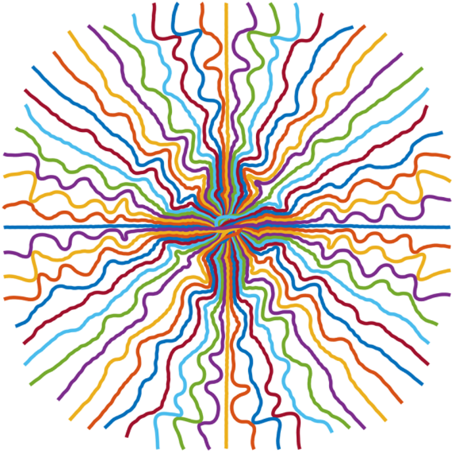

Knee

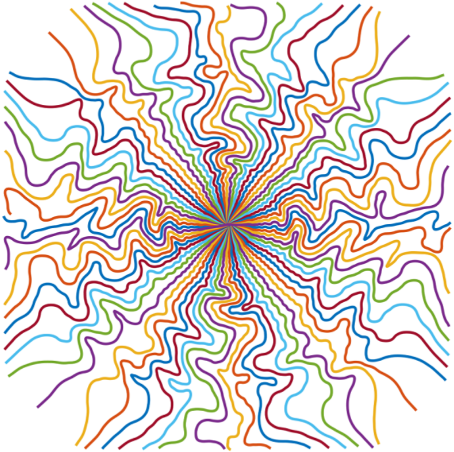

Brain

PSF results: 32 spokes

32-spoke results

FWHM (pixels):

1.5

2.1

1.6

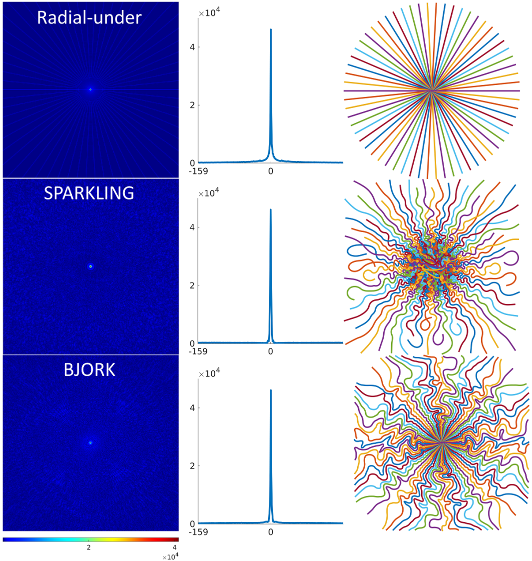

Learning about spectral conjugate symmetry

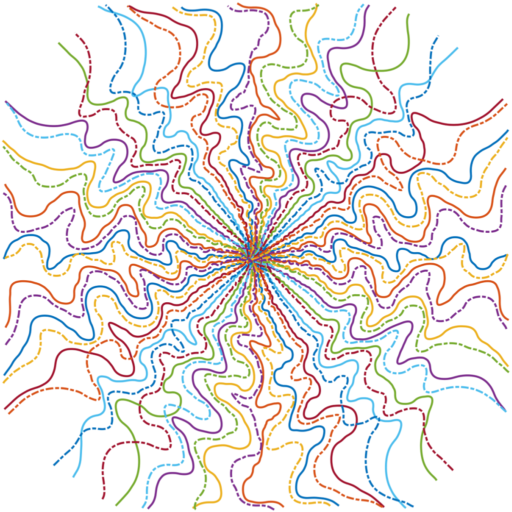

Prospectively under-sampled MRI phantom study

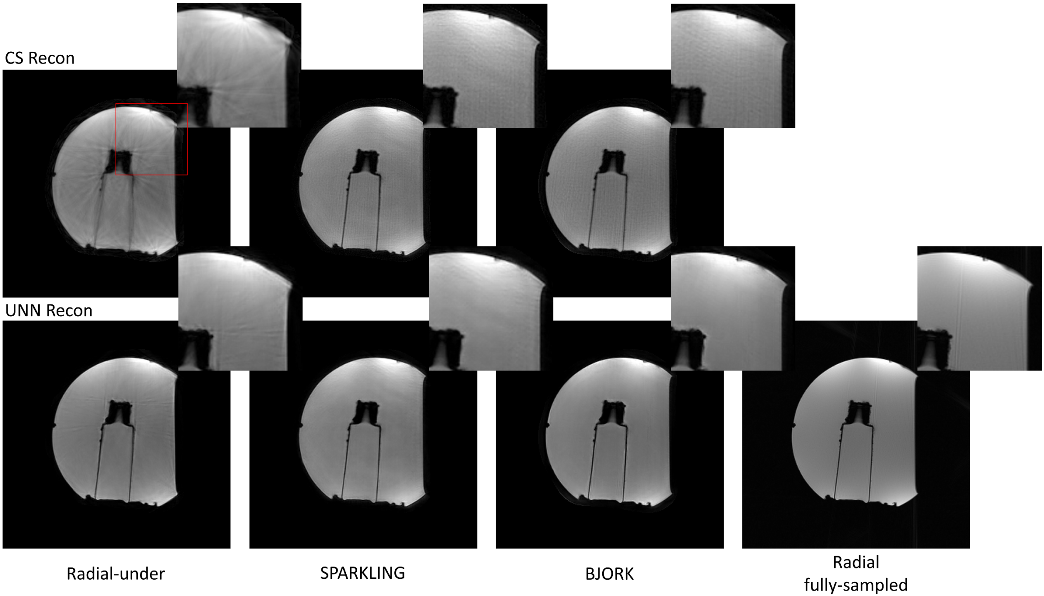

Prospective in-vivo study (GE scanner, 32 shot)

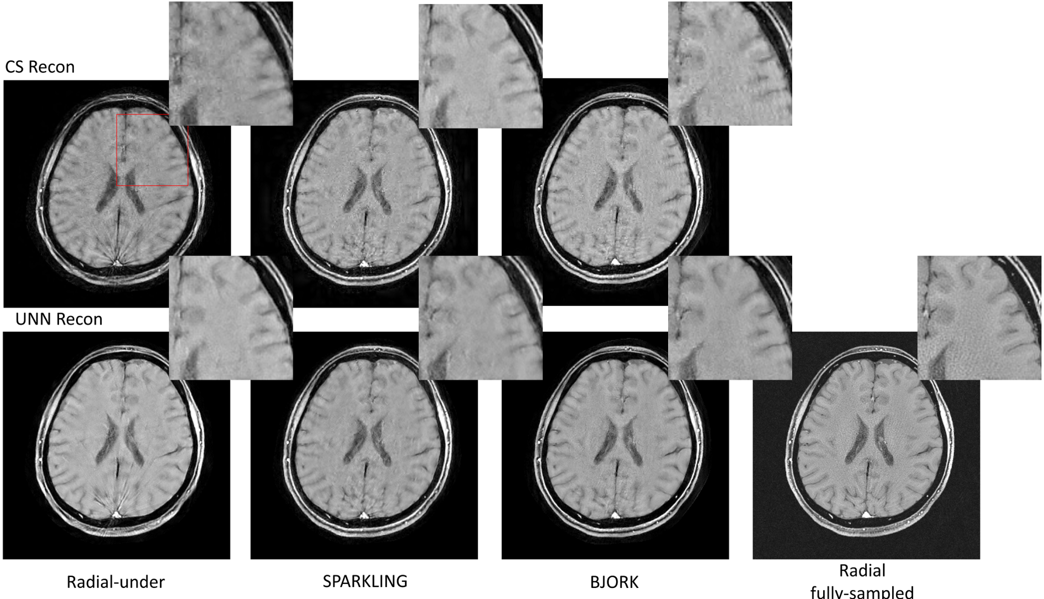

Quantitative simulation results: PSNR

PSNR (in dB):

		Standard	SPARKLING	BJORK
radial-like Ns=16	UNN	32.7	33.9	**34.3**
	CS	31.7	33.6	**34.1**
radial-like Ns=24	UNN	34.1	35.0	**35.6**
	CS	33.3	34.6	**35.1**
radial-like Ns=32	UNN	35.0	36.0	**36.9**
	CS	33.9	35.7	**36.3**
spiral-like Ns=8	UNN	40.9	41.7	**41.9**
	CS	39.9	40.4	**40.7**

Ns: the number of shots or spokes.

Quantitative simulation results: SSIM

SSIM:

		Standard	SPARKLING	BJORK
radial-like Ns=16	UNN	0.940	0.946	**0.950**
	CS	0.911	0.936	**0.938**
radial-like Ns=24	UNN	0.950	0.955	**0.959**
	CS	0.929	0.943	**0.948**
radial-like Ns=32	UNN	0.957	0.963	**0.968**
	CS	0.932	0.946	**0.956**
spiral-like Ns=8	UNN	0.986	0.989	**0.990**
	CS	0.976	0.978	**0.981**

Gradient constraints

MRI gradient amplifiers have maximum amplitude and slew rate

- gradient amplitude is 1st derivative of k-space trajectory:

$$\left\| \boldsymbol{D}_1 \boldsymbol{\omega}_d \right\|_\infty \leq g_{\max}$$

- slew rate is 2nd derivative of k-space trajectory:

$$\left\| \boldsymbol{D}_2 \boldsymbol{\omega}_d \right\|_\infty \leq s_{\max}$$

- Box constraints relaxed to penalty functions that rise rapidly above 1, on:

$$\left\| \boldsymbol{D}_1 \boldsymbol{\omega}_d \right\|_\infty / g_{\max} \text{ and } \left\| \boldsymbol{D}_2 \boldsymbol{\omega}_d \right\|_\infty / s_{\max}$$

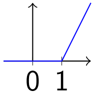

Facilitates (sub)gradient-based optimization using Adam

Trajectory calibration

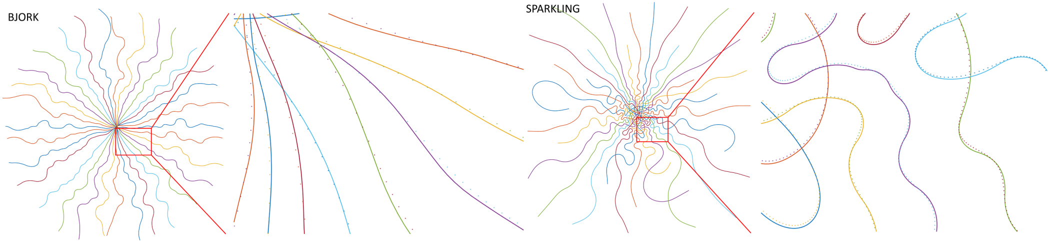

Eddy current compensation

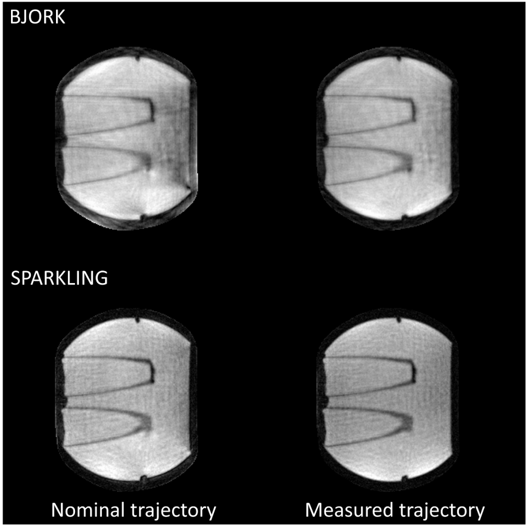

Quadratic B-spline kernels for non-Cartesian k-space trajectory:

$$\boldsymbol{\omega}_d = \boldsymbol{B}\boldsymbol{c}_d, \qquad d = 1, 2, \boldsymbol{c}_d \in \mathbb{R}^{M/\text{Decim}}$$

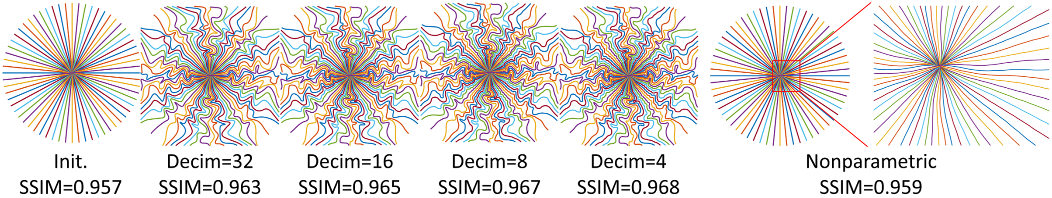

Highly non-convex problem in $\boldsymbol{\omega}$.

- Coarse-to-fine search may find better local minimizers
- However, parameterization/decimation does not save much computation

Motivated by model-based image reconstruction with variable splitting of the form

$$\begin{aligned}\hat{\boldsymbol{x}} &= \arg\min_{\boldsymbol{x}} \|\boldsymbol{A}(\boldsymbol{\omega})\boldsymbol{x} - \boldsymbol{y}\|_2^2 + R(\boldsymbol{x}) \\ &= \arg\min_{\boldsymbol{x}} \min_{\boldsymbol{z}} \|\boldsymbol{A}(\boldsymbol{\omega})\boldsymbol{x} - \boldsymbol{y}\|_2^2 + R(\boldsymbol{z}), \quad \text{s.t. } \boldsymbol{z} = \boldsymbol{x}\end{aligned}$$

Alternating minimization:

$$\begin{aligned}\boldsymbol{x}_{t+1} &= \arg\min_{\boldsymbol{x}} \|\boldsymbol{A}(\boldsymbol{\omega})\boldsymbol{x} - \boldsymbol{y}\|_2^2 + \mu \|\boldsymbol{x} - \boldsymbol{z}_t\|_2^2 && \text{(data consistency, solved via CG)} \\ \boldsymbol{z}_{t+1} &= \arg\min_{\boldsymbol{z}} R(\boldsymbol{z}) + \mu \|\boldsymbol{x}_{t+1} - \boldsymbol{z}\|_2^2 && \text{(denoising)} \\ \text{``} &= \text{''} \mathcal{D}_{\boldsymbol{\theta}}(\boldsymbol{x}_{t+1}) && \text{(CNN denoiser)}\end{aligned}$$

- CNN weights $\boldsymbol{\theta}$ shared across iterations, per MODL [52]
- 6 outer iterations for results shown, with augmented Lagrangian parameter $\mu = 2$

Efficient NUFFT backpropagation I

Training:

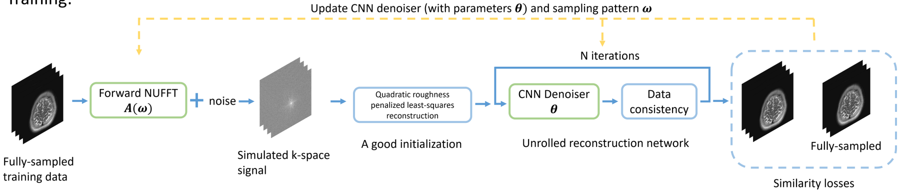

Data consistency block has steps like

$$\boldsymbol{x}_{t+1} = \boldsymbol{x}_t + \alpha \left(\boldsymbol{A}'(\boldsymbol{\omega}) \left(\boldsymbol{A}(\boldsymbol{\omega}) \boldsymbol{x} - \boldsymbol{y} \right) + \mu (\boldsymbol{x} - \boldsymbol{z}_t) \right)$$

$\boldsymbol{A}(\boldsymbol{\omega})$ is dense and huge:

$$a_{ij} = \mathrm{e}^{-\imath \vec{\omega}_i \cdot \vec{r}_j} \tag{1}$$

- Fast approach to $\boldsymbol{A}(\boldsymbol{\omega})\boldsymbol{x}$ uses NUFFT approximation:
  zero-padding, over-sampled FFT, interpolation [65, 66].
- Backpropagation for $\boldsymbol{\omega}$ update through NUFFT steps via autodifferentiation is slow.

Efficient NUFFT backpropagation II

Derive Jacobian matrix for exact form (1):

$$\frac{\partial}{\partial \boldsymbol{\omega}_d} \boldsymbol{A}(\boldsymbol{\omega}) \boldsymbol{x} = -\imath \, \mathrm{Diag}\{\boldsymbol{A}(\boldsymbol{\omega})(\boldsymbol{x} \odot \boldsymbol{r}_d)\}\,.$$

Applying this Jacobian to a vector $\boldsymbol{v} \in \mathbb{C}^M$ during backpropagation yields

$$\left(\frac{\partial}{\partial \boldsymbol{\omega}_d} \boldsymbol{A}(\boldsymbol{\omega}) \boldsymbol{x}\right) \boldsymbol{v} = -\imath \, \mathrm{Diag}\{\boldsymbol{A}(\boldsymbol{\omega})(\boldsymbol{x} \odot \boldsymbol{r}_d)\} \, \boldsymbol{v} = -\imath \, (\boldsymbol{A}(\boldsymbol{\omega})(\boldsymbol{x} \odot \boldsymbol{r}_d)) \odot \boldsymbol{v}\,.$$

Implemented efficiently using NUFFT applied to $\boldsymbol{x} \odot \boldsymbol{r}_d$

Similar idea for Jacobian of adjoint of $\boldsymbol{A}$.
Even more important is accurately approximating Jacobian of CG solve of $(\boldsymbol{A}'\boldsymbol{A} + \mu \boldsymbol{I})^{-1}$

Evolution with improved Jacobians

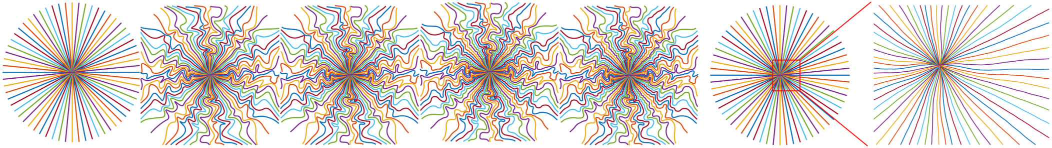

Init.	Decim=32	Decim=16	Decim=8	Decim=4	Nonparametric
SSIM=0.957	SSIM=0.963	SSIM=0.965	SSIM=0.967	SSIM=0.968	SSIM=0.959

Different acceleration factors:

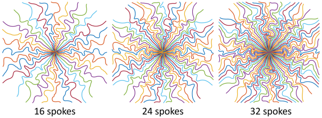

Cross-contrast comparison

- Each contrast has 4500 training slices, 500 test slices
- No extra noise in training
- Testing variance is 10^{-3} mean test signal

SSIM values

test \ training	T1w	T2w	FLAIR
T1w+noise	0.981	0.980	0.981
T2w+noise	0.951	0.953	0.953
FLAIR+noise	0.974	0.974	0.975

Outline

- Machine learning methods have much potential for both scan design and image reconstruction
- Quantitative results in paper demonstrate synergy of jointly optimizing both
- Anatomy specific trajectories: pro or con?
- Self-supervised methods when training data unavailable
- Extension to 3D is in progress
  Also control of peripheral nerve stimulation (PNS)
- Extension to 3D+time is planned (and challenging)

2D code for BJORK: `https://github.com/guanhuaw/Bjork`

Resources

Talk and code available online at
`http://web.eecs.umich.edu/~fessler`

Bibliography I

[1] H. Greenspan, B. van Ginneken, and R. M. Summers. "Guest editorial deep learning in medical imaging: overview and future promise of an exciting new technique." In: *IEEE Trans. Med. Imag.* 35.5 (May 2016), 1153–9.

[2] G. Litjens, T. Kooi, B. E. Bejnordi, A. A. A. Setio, F. Ciompi, M. Ghafoorian, J. A. W. M. . . Laak, B. . Ginneken, and C. I. Sanchez. "A survey on deep learning in medical image analysis." In: *Med. Im. Anal.* 42.C (Dec. 2017), 60–88.

[3] G. Wang, M. Kalra, and C. G. Orton. "Machine learning will transform radiology significantly within the next five years." In: *Med. Phys.* 44.6 (June 2017), 2041–4.

[4] V. Cheplygina, M. . Bruijne, and J. P. W. Pluim. "Not-so-supervised: A survey of semi-supervised, multi-instance, and transfer learning in medical image analysis." In: *Med. Im. Anal.* 54 (May 2019), 280–96.

[5] A. Esteva, A. Robicquet, B. Ramsundar, V. Kuleshov, M. DePristo, K. Chou, C. Cui, G. Corrado, S. Thrun, and J. Dean. "A guide to deep learning in healthcare." In: *Nature Medicine* 25.1 (Jan. 2019), 24–9.

[6] X. Yi, E. Walia, and P. Babyn. "Generative adversarial network in medical imaging: A review." In: *Med. Im. Anal.* 58 (Dec. 2019), p. 101552.

[7] J. Bruna, E. Haber, G. Kutyniok, T. Pock, and Rene Vidal. "Special issue on the mathematical foundations of deep learning in imaging science." In: *J. Math. Im. Vision* 62.3 (2020), 277–8.

[8] D. Rueckert and J. A. Schnabel. "Model-based and data-driven strategies in medical image computing." In: *Proc. IEEE* 108.1 (Jan. 2020), 110–24.

[9] A. Maier, C. Syben, T. Lasser, and C. Riess. "A gentle introduction to deep learning in medical image processing." In: *Zeitschrift für Medizinische Physik* 29.2 (May 2019), 86–101.

[10] S. Ravishankar and Y. Bresler. "Adaptive sampling design for compressed sensing MRI." In: *Proc. Int'l. Conf. IEEE Engr. in Med. and Biol. Soc.* 2011, 3751–5.

[11] L. Baldassarre, Y-H. Li, J. Scarlett, B. Gozcu, I. Bogunovic, and V. Cevher. "Learning-based compressive subsampling." In: *IEEE J. Sel. Top. Sig. Proc.* 10.4 (June 2016), 809–22.

[12] B. Gozcu, R. K. Mahabadi, Y-H. Li, E. Ilicak, T. Cukur, J. Scarlett, and V. Cevher. "Learning-based compressive MRI." In: *IEEE Trans. Med. Imag.* 37.6 (June 2018), 1394–406.

[13] G. Godaliyadda, D. H. Ye, M. D. Uchic, M. A. Groeber, G. T. Buzzard, and C. A. Bouman. "A framework for dynamic image sampling based on supervised learning." In: *IEEE Trans. Computational Imaging* 4.1 (Mar. 2018), 1–16.

[14] H. K. Aggarwal and M. Jacob. "J-MoDL: Joint model-based deep learning for optimized sampling and reconstruction." In: *IEEE J. Sel. Top. Sig. Proc.* 14.6 (Oct. 2020), 1151–62.

[15] C. Bahadir, A. Wang, A. Dalca, and M. R. Sabuncu. "Deep-learning-based optimization of the under-sampling pattern in MRI." In: *IEEE Trans. Computational Imaging* 6 (2020), 1139–52.

[16] Y. Cao and D. N. Levin. "Feature-recognizing MRI." In: *Mag. Res. Med.* 30.3 (Sept. 1993), 305–17.

[17] Y. Cao, D. N. Levin, and L. Yao. "Locally focused MRI." In: *Mag. Res. Med.* 34.6 (Dec. 1995), 858–67.

[18] Y. Cao and D. N. Levin. "Using an image database to constrain the acquisition and reconstruction of MR images of the human head." In: *IEEE Trans. Med. Imag.* 14.2 (June 1995), 350–61.

[19] G. Wang, J. C. Ye, K. Mueller, and J. A. Fessler. "Image reconstruction is a new frontier of machine learning." In: *IEEE Trans. Med. Imag.* 37.6 (June 2018), 1289–96.

[20] G. Wang. "A perspective on deep imaging." In: *IEEE Access* 4 (Nov. 2016), 8914–24.

[21] M. T. McCann, K. H. Jin, and M. Unser. "Convolutional neural networks for inverse problems in imaging: A review." In: *IEEE Sig. Proc. Mag.* 34.6 (Nov. 2017), 85–95.

[22] A. Lucas, M. Iliadis, R. Molina, and A. K. Katsaggelos. "Using deep neural networks for inverse problems in imaging: Beyond analytical methods." In: *IEEE Sig. Proc. Mag.* 35.1 (Jan. 2018), 20–36.

[23] M. T. McCann and M. Unser. "Biomedical image reconstruction: from the foundations to deep neural networks." In: *Found. & Trends in Sig. Pro.* 13.3 (2019), 283–359.

[24] S. Arridge, P. Maass, O. Oktem, and C-B. Schonlieb. "Solving inverse problems using data-driven models." In: *Acta Numerica* 28 (May 2019), 1–174.

[25] V. Monga, Y. Li, and Y. C. Eldar. "Algorithm unrolling: interpretable, efficient deep learning for signal and image processing." In: *IEEE Sig. Proc. Mag.* 38.2 (Mar. 2021), 18–44.

[26] S. Ravishankar, J. C. Ye, and J. A. Fessler. "Image reconstruction: from sparsity to data-adaptive methods and machine learning." In: *Proc. IEEE* 108.1 (Jan. 2020), 86–109.

[27] G. Ongie, A. Jalal, C. A. M. R. G. Baraniuk, A. G. Dimakis, and R. Willett. "Deep learning techniques for inverse problems in imaging." In: *IEEE J. Sel. Areas Info. Theory.* (2020).

[28] E. Haneda, B. Claus, P. FitzGerald, G. Wang, and B. De Man. "CT sinogram analysis using deep learning." In: *Proc. 5th Intl. Mtg. on Image Formation in X-ray CT*. 2018, 419–22.

[29] Q. De Man, E. Haneda, B. Claus, P. Fitzgerald, B. De Man, G. Qian, H. Shan, J. Min, M. Sabuncu, and G. Wang. "A two-dimensional feasibility study of deep learning-based feature detection and characterization directly from CT sinograms." In: *Med. Phys.* 46.12 (Dec. 2019), e790–800.

[30] G. Wang, T. Luo, J-F. Nielsen, D. C. Noll, and J. A. Fessler. *B-spline parameterized joint optimization of reconstruction and k-space trajectories (BJORK) for accelerated 2D MRI*. 2021.

[31] G. Wang, T. Luo, J-F. Nielsen, D. C. Noll, and J. A. Fessler. "B-spline parameterized joint optimization of reconstruction and k-space trajectories (BJORK) for accelerated 2D MRI." In: *IEEE Trans. Med. Imag.* 41.9 (Sept. 2022), 2318–30.

[32] T. Weiss, O. Senouf, S. Vedula, O. Michailovich, M. Zibulevsky, and A. Bronstein. *PILOT: Physics-informed learned optimal trajectories for accelerated MRI*. 2019.

[33] S. Wang, Z. Su, L. Ying, X. Peng, and D. Liang. "Exploiting deep convolutional neural network for fast magnetic resonance imaging." In: *Proc. Intl. Soc. Mag. Res. Med.* 2016, p. 1778.

[34] D. Lee, J. Yoo, and J. C. Ye. *Deep artifact learning for compressed sensing and parallel MRI*. 2017.

[35] K. H. Jin, M. T. McCann, E. Froustey, and M. Unser. "Deep convolutional neural network for inverse problems in imaging." In: *IEEE Trans. Im. Proc.* 26.9 (Sept. 2017), 4509–22.

[36] M. Akcakaya, S. Moeller, S. Weingartner, and Kamil Ugurbil. "Scan-specific robust artificial-neural-networks for k-space interpolation (RAKI) reconstruction: Database-free deep learning for fast imaging." In: *Mag. Res. Med.* 81.1 (Jan. 2019), 439–53.

[37] Y. Han and J. C. Ye. "K-space deep learning for accelerated MRI." In: *IEEE Trans. Med. Imag.* 39.2 (Feb. 2020), 377–86.

[38] M. U. Ghani and W. C. Karl. *Data and image prior integration for image reconstruction using consensus equilibrium*. 2020.

[39] B. Zhu, J. Z. Liu, S. F. Cauley, B. R. Rosen, and M. S. Rosen. "Image reconstruction by domain-transform manifold learning." In: *Nature* 555 (Mar. 2018), 487–92.

[40] I. Haggstrom, C. R. Schmidtlein, G. Campanella, and T. J. Fuchs. "DeepPET: A deep encoder-decoder network for directly solving the PET image reconstruction inverse problem." In: *Med. Im. Anal.* 54 (May 2019), 253–62.

[41] W. Whiteley, W. K. Luk, and J. Gregor. "DirectPET: full-size neural network PET reconstruction from sinogram data." In: *J. Med. Im.* 7.3 (Feb. 2020), 1–16.

[42] W. Whiteley, V. Panin, C. Zhou, J. Cabello, D. Bharkhada, and J. Gregor. "FastPET: near real-time reconstruction of PET histo-image data using a neural network." In: *IEEE Trans. Radiation and Plasma Med. Sci.* 5.1 (Jan. 2021), 65–77.

[43] Y. Yang, J. Sun, H. Li, and Z. Xu. "Deep ADMM-net for compressive sensing MRI." In: *Neural Info. Proc. Sys.* 2016, 10–18.

[44] K. Hammernik, T. Klatzer, E. Kobler, M. P. Recht, D. K. Sodickson, T. Pock, and F. Knoll. "Learning a variational network for reconstruction of accelerated MRI data." In: *Mag. Res. Med.* 79.6 (June 2018), 3055–71.

[45] J. Schlemper, J. Caballero, J. V. Hajnal, A. N. Price, and D. Rueckert. "A deep cascade of convolutional neural networks for dynamic MR image reconstruction." In: *IEEE Trans. Med. Imag.* 37.2 (Feb. 2018), 491–503.

[46] T. M. Quan, T. Nguyen-Duc, and W-K. Jeong. "Compressed sensing MRI reconstruction using a generative adversarial network with a cyclic loss." In: *IEEE Trans. Med. Imag.* 37.6 (June 2018), 1488–97.

[47] D. Lee, J. Yoo, S. Tak, and J. C. Ye. "Deep residual learning for accelerated MRI using magnitude and phase networks." In: *IEEE Trans. Biomed. Engin.* 65.9 (Sept. 2018), 1985–95.

[48] G. Nataraj and R. Otazo. "Investigating robustness to unseen pathologies in model-free deep multicoil reconstruction." In: *ISMRM Workshop on Data Sampling and Image Reconstruction*. 2020.

[49] G. Yang, S. Yu, H. Dong, G. Slabaugh, P. L. Dragotti, X. Ye, F. Liu, S. Arridge, J. Keegan, Y. Guo, and D. Firmin. "DAGAN: Deep de-aliasing generative adversarial networks for fast compressed sensing MRI reconstruction." In: *IEEE Trans. Med. Imag.* 37.6 (June 2018), 1310–21.

[50] K. He, X. Zhang, S. Ren, and J. Sun. "Deep residual learning for image recognition." In: *Proc. IEEE Conf. on Comp. Vision and Pattern Recognition*. 2016, 770–8.

[51] K. Zhang, W. Zuo, Y. Chen, D. Meng, and L. Zhang. "Beyond a Gaussian denoiser: residual learning of deep CNN for image denoising." In: *IEEE Trans. Im. Proc.* 26.7 (July 2017), 3142–55.

[52] H. K. Aggarwal, M. P. Mani, and M. Jacob. "MoDL: model-based deep learning architecture for inverse problems." In: *IEEE Trans. Med. Imag.* 38.2 (Feb. 2019), 394–405.

[53] I. Y. Chun, Z. Huang, H. Lim, and J. A. Fessler. "Momentum-Net: Fast and convergent iterative neural network for inverse problems." In: *IEEE Trans. Patt. Anal. Mach. Int.* (2021). To appear.

[54] P. Putzky, D. Karkalousos, J. Teuwen, N. Miriakov, B. Bakker, M. Caan, and M. Welling. *i-RIM applied to the fastMRI challenge*. 2019.

[55] F. Knoll, T. Murrell, A. Sriram, N. Yakubova, J. Zbontar, M. Rabbat, A. Defazio, M. J. Muckley, D. K. Sodickson, C. L. Zitnick, and M. P. Recht. "Advancing machine learning for MR image reconstruction with an open competition: Overview of the 2019 fastMRI challenge." In: *Mag. Res. Med.* 84.6 (Dec. 2020), 3054–70.

[56] M. J. Muckley, B. Riemenschneider, A. Radmanesh, S. Kim, G. Jeong, J. Ko, Y. Jun, H. Shin, D. Hwang, M. Mostapha, S. Arberet, D. Nickel, Z. Ramzi, P. Ciuciu, J-L. Starck, J. Teuwen, D. Karkalousos, C. Zhang, A. Sriram, Z. Huang, N. Yakubova, Y. W. Lui, and F. Knoll. "Results of the 2020 fastMRI Challenge for Machine Learning MR Image Reconstruction." In: *IEEE Trans. Med. Imag.* 40.9 (Sept. 2021), 2306–17.

[57] J. Huang, Y. Fang, Y. Nan, H. Wu, Y. Wu, Z. Gao, Y. Li, Z. Wang, P. Lio, D. Rueckert, Y. C. Eldar, and G. Yang. *Data and physics driven learning models for fast MRI – fundamentals and methodologies from CNN, GAN to attention and transformers*. Submitted to ieee-spmag. 2022.

[58] M. Seeger, H. Nickisch, R. Pohmann, and B. Schölkopf. "Optimization of k-space trajectories for compressed sensing by Bayesian experimental design." In: *Mag. Res. Med.* 63.1 (Jan. 2010), 116–26.

[59] G. Wang, T. Luo, J-F. Nielsen, J. A. Fessler, and D. C. Noll. "B-spline parameterized joint optimization of reconstruction and K-space sampling patterns (BJORK) for accelerated 2D acquisition." In: *Proc. Intl. Soc. Mag. Res. Med.* 2021, p. 0833.

[60] G. Wang and J. A. Fessler. *Efficient approximation of Jacobian matrices involving a non-uniform fast Fourier transform (NUFFT)*. 2021.

[61] G. Wang and J. A. Fessler. "Efficient approximation of Jacobian matrices involving a non-uniform fast Fourier transform (NUFFT)." In: *IEEE Trans. Computational Imaging* (2021). Submitted.

[62] S. Yu, B. Park, and J. Jeong. "Deep iterative down-up CNN for image denoising." In: *Proc. IEEE Conf. on Comp. Vision and Pattern Recognition*. 2019, 2095–103.

[63] G. Wang, D. C. Noll, and J. A. Fessler. "Efficient NUFFT backpropagation for stochastic sampling optimization." In: *Proc. Intl. Soc. Mag. Res. Med.* 2021, p. 0913.

[64] C. Lazarus, P. Weiss, N. Chauffert, F. Mauconduit, L. El Gueddari, C. Destrieux, I. Zemmoura, A. Vignaud, and P. Ciuciu. "SPARKLING: variable-density k-space filling curves for accelerated T2*-weighted MRI." In: *Mag. Res. Med.* 81.6 (June 2019), 3643–61.

[65] A. Dutt and V. Rokhlin. "Fast Fourier transforms for nonequispaced data." In: *SIAM J. Sci. Comp.* 14.6 (Nov. 1993), 1368–93.

Bibliography VII

[66] J. A. Fessler and B. P. Sutton. "Nonuniform fast Fourier transforms using min-max interpolation." In: *IEEE Trans. Sig. Proc.* 51.2 (Feb. 2003), 560–74.